

## NEAR-CRITICAL POINT HYDRODYNAMICS AND MICROGRAVITY

Daniel A. Beysens

*CEA, Service des Basses Températures, Grenoble &  
ESPCI, PMMH, 10, rue Vauquelin, 75015, Paris Cedex 05, France*  
dbeysens@cea.fr

**Abstract** Near their critical point, fluids exhibit anomalous behavior of thermodynamic parameters (divergence of specific heat, compressibility and expansion coefficients) and transport coefficients (heat conductivity, thermal diffusivity). Weightlessness ("microgravity") environment permits to go very close to the critical point, thus allowing key tests of the Renormalization Group theory to be made. It also results in a very particular hydrodynamics of dense and hyper-compressible gases, where weightlessness experiments play a key role. For instance, a very fast thermalization effect ("Piston effect") is evidenced, where a thermal boundary layer expands and adiabatically heats the whole fluid, leading in some cases to an (apparent) violation of the laws of thermodynamics. Another one is concerned with the use of critical slowing down and microgravity to investigate the dynamics of phase separation with no gravity-induced sedimentation. The key role of the coalescence of domains makes valid only two simple growth laws; they can be successfully applied to a quite different situation, the evolution laws in the well-known biological problem of sorting of the embryonic cells. Other situations are concerned with the effect of vibrations. The investigation of the above thermal and phase transition problems suggest that a periodic excitation can act as a kind of artificial gravity, which induces thermal convection, speeds up phase transition and localizes the liquid and vapor phases perpendicular to it. Some of these phenomena still persist at higher temperature and pressure. Fluids in such supercritical conditions are very appealing to the industry as non-polluting solvents or hosts of chemical reactions with high yield.

**Keywords:** Critical point, supercritical fluids, phase transition, thermalization, cell sorting, Piston effect, microgravity, vibrations, cell sorting

## 1. Introduction

It is widely believed that a fluid can exist only as a gas or a liquid. However, there is another state, the "supercritical state", that fluids can exhibit (Fig. 1a). Since Baron Charles Cagniard de La Tour discovered in 1821 that the liquid and gas phases of a carbon dioxide sample became undistinguishable after crossing a "critical" temperature of  $31^{\circ}\text{C}$  and a "critical" pressure of 72 bar, the intriguing properties of this very particular state has motivated a great number of studies.

The critical point co-ordinates vary according to the particular fluid under study. For instance, the critical point of carbon dioxide ( $\text{CO}_2$ ) is observed at  $31^{\circ}\text{C}$  and 72 bar, that of water ( $\text{H}_2\text{O}$ ) at  $375^{\circ}\text{C}$  and 225 bar and that of hydrogen ( $\text{H}_2$ ) at 33 K and 13 bar. Above the critical temperature and pressure, supercritical fluids exhibit a number of specific properties (large density, low viscosity, large diffusivity) which make them intermediate between liquids and gases [1]. In addition, their isothermal compressibility and thermal expansion can become very large, especially when they approach the critical point. The highly variable properties of near-critical fluids make them very attractive for studying many phenomena that hold for all fluids because of the critical universality. Supercritical fluids are increasingly used by the food and waste management industry [3] for their solubilization properties (e.g. supercritical  $\text{CO}_2$ ), as host of "cold" combustion (e.g. supercritical water), in energetics (supercritical thermal or nuclear plants), and in astronautics (e.g. storage of cryogenic fluids).

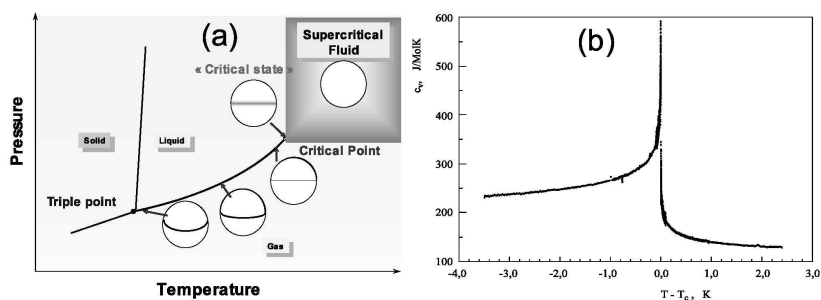


Figure 1. (a): Phase diagram of a pure substance. The supercritical "state" corresponds to a compressed gas that exhibits the density of a liquid. (b): Critical anomaly of the specific heat at constant volume ( $C_v$ ) measured under zero-gravity in  $\text{SF}_6$  (Spacelab D2, 1993). (From [2]).

## Near-critical Fluids and Microgravity

Fluids in their near-critical or supercritical state are strongly affected by gravity. As they are highly compressible, gravity compresses them under their own weight. The density varies in the sample, thus preventing a close approach to the critical point to be made, cf. [4].

They exhibit anomalies in the transport of heat so that convection and buoyancy phenomena, often turbulent, appear for even minute temperature gradients. We show in the following that space experiment have enabled new phenomena to be discovered thanks to a close approach to the critical point and the removal of convection and buoyancy.

The effects of gravity can be removed in space thanks to spacecrafts and satellites. On earth, microgravity conditions can be obtained during a short time period in a free fall tower (a few s) and in parabolic flights of planes (20 s) and sounding rockets (2–12 min.). Some other means can be used with liquid mixtures. Liquid mixtures near their consolute critical point exhibit a number of common features with pure fluids, when concentration is replaced by density as an order parameter of the transition. Some aspects can be then studied with binary liquid mixtures that have been made density-matched by partial deuteration [5].

The compensation of gravity forces in simple fluids is more difficult. The large diamagnetism susceptibility of  $H_2$  was used to compensate gravity by a magnetic force, proportional to its density. By using a superconducting coil it became possible to study, without gravity effects, the process of solidification and gas-liquid phase transition over a wide range, from the triple point (13.8 K) to above the critical point (33 K) [6]. A vibration device has also been implemented using a special sapphire sample.

## 2. Universality and Scaling Laws

An important aspect of the critical region is that most of the anomalies of the thermodynamic and transport properties can be set in the form of scaled, universal (power law) functions with respect to the critical point (CP) coordinates. Then, any results obtained with one single fluid can be immediately generalized to a whole class of systems, the "class of fluids", to which belong also liquid mixtures, including polymer melts and solutions, microemulsions, molten salts, monotectic liquid metals, etc. [1]. This scaling is of fundamental nature and stems from the universal behavior that the free energy must asymptotically obey to fulfill the conditions of a 2nd order phase transition – the CP. In a sense, scaling is generic to CP phenomena. By permitting the measurements to be extremely close to the critical point, zero-g experiments

have made possible the precise measurements of important, weak power-law divergence, such as that of the specific heat at constant volume  $C_v$  (Fig. 1-b). From space experiments, the temperature divergence of the specific heat has been determined with a very high precision. With the reduced temperature  $\tau = (T - T_c)/T_c$  ( $T$  is temperature,  $T_c$  is the absolute critical temperature), the specific heat diverges as  $C_v \sim \tau^{-\alpha}$  near the critical point. The "critical" exponent  $\alpha$  is universal. Its precise determination was a key test of the 'Renormalization Group' theory, which has been developed in order to try to improve the classical macroscopic description of fluid behavior close to the critical point [7]. The value deduced from the space experiments,  $\alpha = 0.1105 \pm 0.027$  [2], indeed appears to be very close to the result of the Renormalization Group theory,  $\alpha = 0.110 \pm 0.005$ .

### 3. Phase Transition Kinetics and Morphology

Let us describe a typical phase separation experiment (Fig. 2a) and what has been learned from the space experiments [9]–[10]. The supercritical fluid is thermally quenched from a region of the phase diagram where it is homogeneous (at temperature  $T_i$ ) to a region where it is thermodynamically stable as two phases (at temperature  $T_f$ ). Droplets nucleate and their development is limited by coalescence events. When the volume fraction of the new phase that has nucleated is low (Fig. 2b), the droplets collide by Brownian motion and coalesce. The average radius of the drops  $R$  or the average distance  $L_m$  between them evolves as

$$R\phi^{-1/3} \sim L_m = 2\pi(k_B T/6\pi\eta)t^{1/3}, \quad (1)$$

where  $t$  is time,  $\eta$  is the shear viscosity,  $T$  is absolute temperature and  $k_B$  is the Boltzmann constant. It is worth noting that this law is practically independent of the distance  $(T - T_c)$  from the critical point.

To a given  $\phi$  corresponds a typical interaction length ( $\approx R/3$ ) between domains. When  $\phi > 0.3$ , it is found [10] that the flow generated by a coalescence event is able to move a neighboring drop and thus induces another coalescence. Such a process therefore creates a chain reaction of coalescence. In the viscous limit, the pattern looks to be interconnected. Growth is limited by the balance between the capillary pressure gradient  $\sigma/R$  ( $\sigma$  is the gas-liquid surface tension) and the friction due to the shear viscosity, so that (late times)

$$L_m = b(\sigma/\eta)t. \quad (2)$$

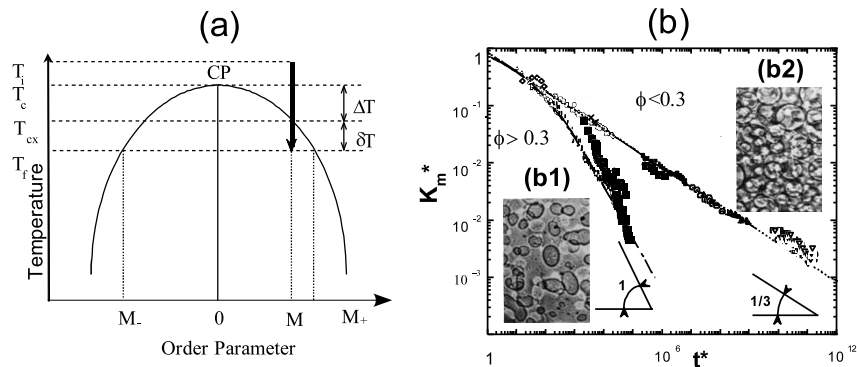
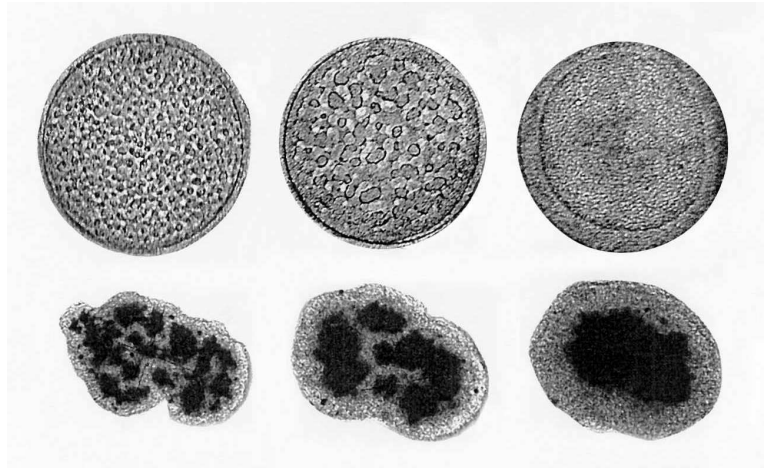


Figure 2. (a): Schematic phase diagram for simple fluids and liquid mixtures in the plane  $T - M$ . CP: critical point.  $T$ : temperature.  $M$ : order parameter;  $M = (\rho/\rho_c) - 1$  for simple fluids and  $M = c - c_c$  for liquid mixtures.  $\rho(\rho_c)$  is density (critical density).  $c(c_c)$  is concentration (critical concentration). The coexistence curve is described by  $M = B\tau^\beta$  with  $B$  being a system-dependent amplitude and  $\beta = 0.325$  an universal exponent. (b): Growth laws when gravity effects are absent. Fluids ( $SF_6, CO_2$ ): all data points except open squares. Liquid mixtures (partially deuterated Cyclohexane and Methanol): letters and open squares. The evolution of the average distance between the domains ( $L_m$ ) is expressed in the scaled units  $K_m^* = 2\pi\xi/L_m$  and  $t^* = t/t_\xi$  (see text). Lines are theoretical predictions. The lower curve ( $\phi > 0.3$ ) corresponds to a "fast" growth law and an interconnected morphology (pattern in insert b1) and the reduced upper curve ( $\phi < 0.3$ ) refers to a "slow" growth and a disconnected morphology (pattern in insert b2). (From Ref. [9]).

Here  $b \approx 0.03$  is a universal constant. All experiments can be rescaled by the natural lengthscale and timescale: the correlation length  $\xi$  of density fluctuations ( $\xi$  diverges as  $\tau^{-\nu}$ ), and the associated diffusion time  $t_\xi$  ( $t_\xi$  diverges as  $\tau^{-3\nu}$ ).

## Application to Biological Tissues

The development of domains by coalescence events, as reported above, is very general. The universality of behavior, which is observed in fluids and liquid mixtures, can be extended to other areas of science. In particular, it can be applied to developmental biology where tissues can be considered as very viscous liquids (viscosity  $\eta \approx 10^6$  Po), with a surface tension arising from the balance of adhesion sites between the tissue cells (effective interfacial tension  $\sigma \approx 10$  dyn.cm $^{-1}$ ). When analyzing both the kinetics and morphology of cell sorting in embryonic chicken tissues, [11](Fig. 3), the development of the pattern can be interpreted as



*Figure 3.* Upper sequence: gas and liquid phase ordering in  $\text{SF}_6$  under reduced gravity, after a thermal quench to  $T_c - 0.7$  mK. Cell diameter: 12 mm. Gas and liquid eventually order with the liquid phase wetting the container wall and surrounding the gas phase, corresponding to  $\sigma_{wl} < \sigma_{wg}$ . Here  $\sigma_{wl}$  and  $\sigma_{wg}$  are the wall-liquid and wall-gas interfacial tensions, respectively. The three pictures from the left correspond to states at 120 s, 275 s and 3960 s after quench, respectively. Lower sequence: sorting out of chicken embryonic pigmented epithelial cells (dark) from chicken embryonic neural retinal cells (light). Aggregate size:  $200 \mu\text{m}$ . At the end of sorting, neural retinal cells preferentially wet the external tissue culture medium surrounding the aggregates. Here  $\sigma_{tn} (=1.6 \text{ dyn/cm}) < \sigma_{tp} (=12.6 \text{ dyn/cm})$ , where  $\sigma_{tn}$  and  $\sigma_{tp}$  are the tissue culture medium-neural retina and the tissue culture medium-pigmented epithelium interfacial tensions, respectively. The three pictures from the left correspond to 17 h, 42 h and 73 h after initiation of sorting, respectively. (From [11]).

a result of the coalescence of domains that rearrange like droplets. The domains continuously coalesce and form a network, showing the same linear evolution as the fast growth in liquids. The pseudo-period between domains can indeed be fitted to a linear growth law  $L_m = bt$ . The value of parameter  $b$  turns out to be comparable to that extracted from Eq. (2), although surface tension and viscosity values differ by factors as large as  $10^8$ .

#### 4. Thermalization

##### The "Piston" Effect

The thermal diffusivity of fluids vanishes near the critical point and a simple calculation [12] shows that it would need more than one month to reach thermal equilibration in a sample of  $1 \text{ cm}^3$  at  $T - T_c = 1 \text{ mK}$ .

At the beginning of the microgravity experiments, it thus seemed hopeless to the scientists to try to homogenize in temperature and density a sample of fluid close to the critical point in a reasonable experiment time. However, in 1986, a preliminary experiment by Straub in a sounding rocket [8] indicated that thermalization might be much faster than expected. In a workshop in 1989 on thermal equilibration near the critical point, Onuki pointed out the importance of "adiabatic heating". We proposed a hydrodynamic mechanism of thermalization that was based on hydrodynamics where, at the sample wall the hot diffuse boundary layer expands and compresses adiabatically the whole fluid. Thermalization proceeds at the velocity of sound. As a result, a spatially uniform heating of the bulk fluid should be observed. There should be a real flow at the boarder between the bulk fluid and the expanding diffuse layer, later observed under microgravity as real "jet" flows. Onuki and Ferrell and the Gammon team proposed a similar process, an "adiabatic heating". In the Physical Review A issue of December, 1990 [12]-[14] Onuki and Ferrell, the Gammon team and our group exposed their views on the subject and all concluded a fast thermalization by this effect. Other reports (Meyer in [15]) came out nearly at the same time. We coined in [12] this adiabatic heating phenomenon the "Piston Effect" (PE), a name which has been accepted by the scientific community.

### **Can Heat Flow Backwards?**

This effect is at the origin of a very particular behavior [17] when the vapor is in equilibrium with liquid below the critical point (Fig. 4b). While heating the cell, the temperature of the vapor becomes greater than that of the wall. That heat flow could seemingly flow from cold to hot contradicts the laws of thermodynamics. However, as we are here in presence of a thermo-mechanical conversion where the hot boundary layer compresses more the gas than the liquid, the violation is only apparent.

These results concerning the PE have been adapted and modified to the earth's environment, where gravity couples to the PE-induced flows and the geometry of the phases. Paradoxical phenomena, such as the cooling of the bulk fluid after a heat pulse, have also been obtained [18]. Also, the accelerations of the shuttle have been used (rotation and maneuvering the shuttle) to investigate the effect of density destratification, a study performed with Air Liquide Company to validate the codes that are now used in the pressurization of the reservoirs of the Ariane 5 rocket.

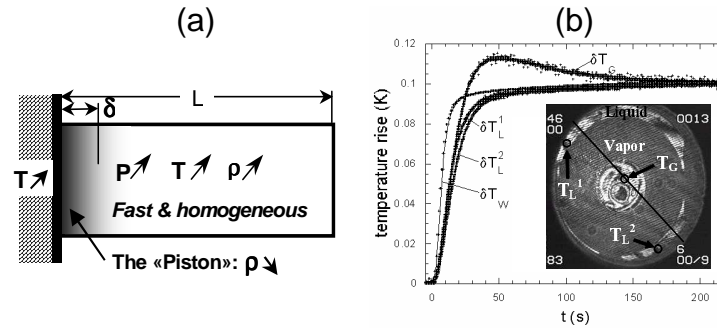


Figure 4. (a): The Piston Effect mechanism [12]-[16]: a thin hot boundary layer expands and compresses the bulk fluid. The corresponding temperature profile shows a thin zone of strong gradients near the heated boundary (thermal boundary layer  $\delta$ ) and a homogeneous rise in the rest of the fluid, that settles at the speed of sound. (b): overheating of nearly 20% obtained in the gas phase of a  $SF_6$  sample at 10 K below the critical point (ALICE in MIR, 1999). A temperature rise of  $T_w = 0.1K$  is imposed at the cell wall. The temperature evolution of the gas ( $\delta T_G$ ), that of the liquid ( $\delta T_L$ , at two locations) are shown. In the insert is reported the sample with the thermistors. The fact that heat can flow from “cold” to “hot” apparently violates thermodynamics. It is a spectacular demonstration of the reality of the “piston” in the “Piston Effect”. (From Ref.[17]).

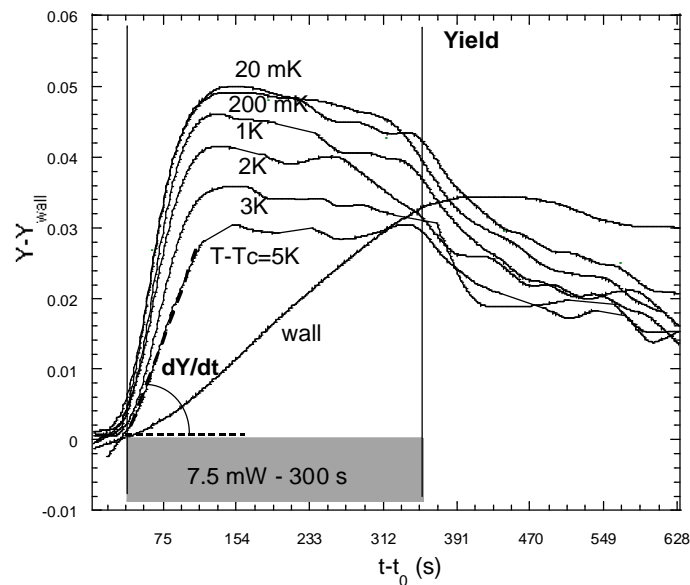


Figure 5. Yield  $Y = \text{transmitted power} / \text{incident power}$  vs time (s) at various  $T - T_c$ . Fluid is  $H_2$  ( $T_c = 33K$ ). At time  $t_0$ , power (7.5 mW) is sent for 300 s at one end of the cell. The transmitted power is measured at the other end. The conduction  $Y_{wall}$  by the wall of the sample cell (curve “wall”) has been subtracted.

Since temperature outside the thermal boundary layers is homogeneous, the bulk fluid acts as a thermal short circuit. A question arises whether it is possible to use this Piston effect as a kind of heat pipe to carry heat on long distances. Experiments and simulation have been performed with  $H_2$  [19] in a magnetic gravity compensation set-up [6]. The results (Fig.5) show that the heat transfer is very fast, in contrast to the usual conduction process. In particular, the yield  $Y$  (see Fig. 5 caption) shows a finite slope at initial time, in contrast with conduction in the cell walls where the slope is zero. The maximum yield increases when  $T$  approaches  $T_c$ . Its value corresponds to the heat transfer in the steady conduction state (at infinite time).

## 5. High Frequency Vibrations

At high frequency excitation - i.e. frequencies larger than the inverse typical hydrodynamics times - the time average of the Bernoulli pressure, which is proportional to the fluid square velocity, is non-zero. The pressure gradient that appears in a non-homogeneous fluid can thus induce flows perpendicular to the vibration direction. However, at low frequency, vibration acts by its instantaneous acceleration and can induce flows parallel to the vibration (as usually gravity does). In the following,  $a$  will denote the vibration amplitude,  $f$  the frequency and  $\omega = 2\pi f$  the angular frequency.

### Vibrational Thermal Effects

When a fluid is submitted to a vibrational acceleration in a thermal gradient in the Rayleigh-Bénard configuration, convection is able to start at conditions corresponding to a vibrational Rayleigh number [20]

$$Rav = \frac{[a\omega(\partial\rho/\partial T)_p\Delta T e]^2}{2\eta D} \quad (3)$$

larger than a few thousands. Here  $\Delta T$  is the temperature difference between two fluid layers separated by the distance  $e$  and  $D$  is the thermal diffusivity coefficient. As the fluid temperature becomes closer to the critical temperature,  $Rav$  diverges as  $(T - T_c)^{-1.9}$ . The fluid then becomes extremely sensitive to vibration as the critical point is approached.

Measurements of flow velocities performed in the MIR station in  $CO_2$  and in  $SF_6$  confirm this expectation [22]-[23] (Fig. 6). A heat flux was sent into the fluid from a point-like source (thermistor). Depending on the oscillation velocity, two regimes of heat propagation are observed: (i) at low frequency, heat is convected during one oscillation period to form plumes parallel to vibration (Fig. 6b); (ii) at high frequency, heat

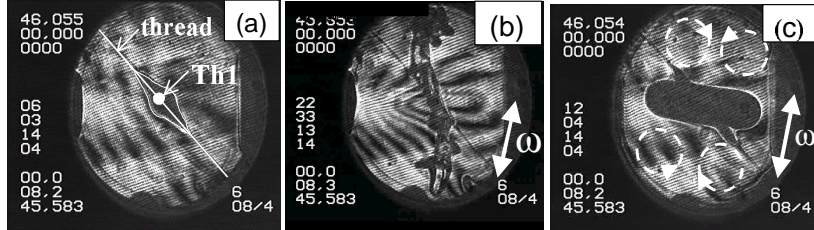


Figure 6. Interferometer image of the hot boundary layer around a heating thermistor *Th1*, supported by a thread. Fluid:  $SF_6$  at  $T_c + 0.5$  K. (a) no vibration (hot region underlined in white); (b) under low frequency; (c) under high frequency vibration. Here convection rolls form. (ALICE in MIR, 1999, from [27]).

is convected by convection rolls perpendicularly to the direction of oscillation (Fig. 6c). A numerical simulation and analysis of the convection has been performed by Jounet in [21], emphasizing the role of vortices.

## Vibrational Phase Ordering

A plane liquid-vapor layer vertically vibrating parallel to gravity displays two different regimes [24]. Far from the critical point, a square wave-pattern deformation arises (the usual Faraday instability). At a temperature  $T_0$  close to the critical temperature ( $T_c - T_0 \approx 20$  mK for  $CO_2$ ), a transition to a new pattern comprised of lines occurs. This transition is due to the increase of dissipation near the critical point. This is a rather unique example of a strong coupling between two different critical point phenomena: the critical point of interface instability and the thermal critical point of the liquid-vapor phase transition.

When acceleration is perpendicular to gravity, a Kelvin-Helmholtz-like instability is observed [25], with the interface modulated as a "frozen" roll wave pattern (Fig. 7a). The mechanism of the instability results from the relative motion of the two fluids induced by vibration. A perturbation becomes unstable if the cell velocity ( $a\omega$ ) is larger than the threshold velocity [26]

$$(a\omega)_0 = \frac{(\rho_L + \rho_G)^3}{\rho_L \rho_G \Delta \rho} \sqrt{\frac{\sigma g}{\Delta \rho}}. \quad (4)$$

Here  $\rho_L$  ( $\rho_V$ ) is the liquid (vapor) density and  $\Delta \rho = \rho_L - \rho_G$  is the liquid-vapor density difference. This destabilization is due to the increasing effect of the Bernoulli - type pressure arising from the velocity difference between gas and liquid.

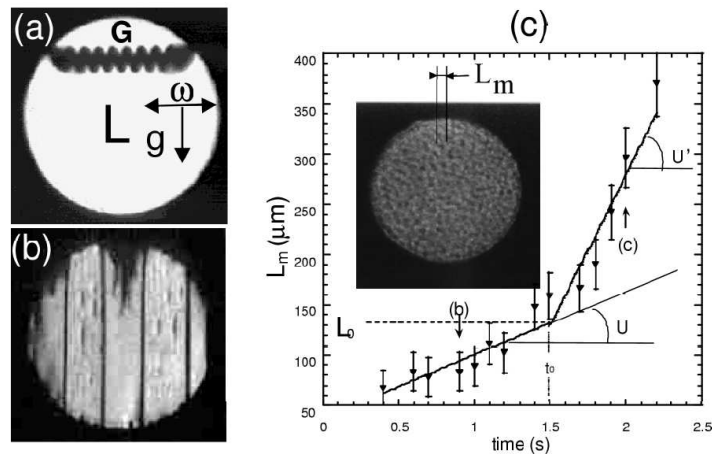


Figure 7. (a-b):  $\text{CO}_2$  gas-liquid phases show up under 1-g as gas phase (G) above the liquid phase (L) separated by a flat meniscus. When submitted to vibration, the phases can order in a different way: (a) under  $1-g$ , the interface exhibits "frozen waves"; (b) under zero-g, gas-liquid phases order in layers. Cell diameter: 10 mm (sounding rocket Maxus 5, April, 2003). (c): Typical phase separation in  $\text{H}_2$  at  $T_c - 1.06 \text{ mK}$  with  $a = 0.3 \text{ mm}$  and  $f = 20 \text{ s}^{-1}$ . From [28].

Three samples of different gas volume fractions and various  $T - T_c$  were vibrated at several amplitudes and frequencies ranging from 0.1 mm to 5 mm and 0.1 Hz to 60 Hz, respectively [27]. Although the initial state of the sample was either an emulsion of vapor drops, or a single drop, the final state remains the same: vapor and gas phases are forming alternate layers perpendicular to the direction of acceleration. An instability, similar to Kelvin-Helmholtz' with inviscid, zero surface tension, develops as liquid fingers from the cell walls. The fingers coalesce with the droplets in the bulk and/or with the fingers that have grown from the opposite side. Here the viscous boundary layer  $\lambda = (2\eta/\rho\omega)^{1/2}$  is the natural lengthscale of the phenomenon.

## Phase Transition under Vibration

A study of phase separation was performed in  $\text{H}_2$  under magnetic compensation of gravity (Fig. 7c), for volume fraction  $\phi > 0.3$  [28]. The domains are interconnected. When  $L_m$  is lower than the viscous boundary layer  $\lambda$ , liquid and gas domains have the same velocity and their growth is unaffected. From Eq. (2), the growth velocity  $U = dL_m/dt = b\sigma/\eta$ . When  $L_m > \lambda$ , the domains exhibit different velocities whose difference is proportional to the gas-liquid difference. The corresponding shear flow

between the domains speeds up the growth (see Fig. 7c where the crossover is denoted  $L_0$ ) as  $U'/U = 1 + \Delta U/U$ , with  $\Delta U/U \sim (\Delta\rho)(a/\lambda)$ .

These observations suggest that a periodic excitation can act as a kind of artificial gravity, which speeds up phase transition and localizes the liquid and vapor phases perpendicular to it.

## 6. Conclusion

Supercritical fluids are of both the fundamental interest (universality of phase transition, supercritical hydrodynamics) and industrial interest (supercritical solubilization, nucleation of nanomaterials, oxidation, thermalization, storage). The field of Critical Point Phenomena has achieved some major breakthroughs during the last 15 years thanks to microgravity research; in particular, a new thermalization process has been discovered, the "Piston Effect", that reveals novel hydrodynamics in such near-critical fluids. The study has strongly modified our vision of critical point phenomena and even of hydrodynamics: the very unusual hydrodynamics of these supercritical fluids, compressible, dense, and weakly viscous, makes their behavior quite particular when compared to gas or liquids. Future experiments will certainly lead to the discovery of new and unexpected phenomena that will be of interest for both the fundamental and applied science.

## Acknowledgments

This review has been made possible thanks to the friendly help and contribution of Y. Garrabos, B. Zappoli, J. Hegseth, P. Evesque and V. Nikolayev. The financial support of CNES is gratefully acknowledged.

## References

- [1] See e.g. H.E. Stanley, *Introduction to phase transitions and critical phenomena*, Clarendon Press, Oxford, New York, 1971; D. Beysens, J. Straub, D. Turner, [in:] *"Fluid Sciences and Materials Science in Space"*, H.U. Walter [Ed.], pp.221–256, Springer, Berlin, 1987.
- [2] A. Haupt, J. Straub, Phys. Rev. E 59, pp.1795–1802, 1999.
- [3] F. Cansell, P. Beslin, B. Berdeu, Environmental Progress 17, pp.258–263, 1998; S. Yesodharan, Current Science 82, pp.1112–1122, 2002.
- [4] M.R. Moldover, J.V. Sengers, R.W. Gammon, R.J. Hocken, Rev. Mod. Phys. 51, pp.79–99, 1979.
- [5] D. Beysens, Acta Astron. 12 525-530, 1985; C. Houessou, P. Guenoun, R. Gastaud, F. Perrot, D. Beysens, Phys. Rev. A 32, pp.1818–1833, 1985.
- [6] R. Wunenburger, D. Chatain, Y. Garrabos, D. Beysens, Phys. Rev.E 62, pp.469–476, 2000; see <http://www.spaceflight.esa.int>.

- [7] K.G. Wilson, J. Kogut, Phys. Reports C 12, 75, 1974.
- [8] K. Nitsche, J. Straub, Naturwissenschaften 73, 370, 1986; J. Straub, L. Eicher, A. Haupt, Phys. Rev. E 51, pp.5556–5563, 1995.
- [9] D. Beysens, Y. Garrabos, Physica A 281, 361-380, 2000 and refs. therein.
- [10] V. Nikolayev, D. Beysens, P. Guenoun, Phys. Rev. Lett. 76, pp.3144–3147, 1996; V. Nikolayev, D. Beysens, Physics of Fluids 9, pp.3227-3234, 1997.
- [11] D.A. Beysens, G. Forgacs, J.A. Glazier, P.N.A.S. 97, pp.9467-71, 2000; *ibid.*, *Networks of droplets induced by coalescence: application to cell sorting*, in: Dynamical Networks in Physics and Biology, D. Beysens and G. Forgacs [Eds.], pp.161–169, Springer & EDP Sciences, Berlin & Les Ulis, 1998.
- [12] B. Zappoli, D. Bailly, Y. Garrabos, B. Le Neindre, P. Guenoun, D. Beysens, Phys. Rev. A 41, pp.2264–2267, 1990.
- [13] A. Onuki, H. Hao, R.A. Ferrell, Phys. Rev.A 41, pp.2255-2259, 1990; A. Onuki, R.A. Ferrell, Physica A 164, pp.245–264, 1990.
- [14] H. Boukari, J.N. Shaumeyer, M.E. Briggs, R.W. Gammon, Phys. Rev. A 41, pp.2260–2263, 1990.
- [15] R.P. Behringer, A. Onuki, H. Meyer, J. Low Temp. Phys. 81, pp.71–102, 1990.
- [16] See e.g. Y. Garrabos, M. Bonetti, D. Beysens, F. Perrot, T. Fröhlich, P. Carlés, B. Zappoli, Phys. Rev. E. 57, pp.5665-5681, 1998.
- [17] R. Wunenburger, Y. Garrabos, C. Chabot, D. Beysens and J. Hegseth, Phys. Rev. Lett. 84, pp.4100–4103, 2000; M. Sincell, Science 288, pp.789–791, 2000.
- [18] T. Fröhlich, D. Beysens, Y. Garrabos, V. Nikolayev, A heat flux can cool a near-critical fluid, preprint, 2004.
- [19] D. Beysens, D. Chatain, V. Nikolayev, Y. Garrabos, 4th International Conference on Launcher Technology *Space Launcher Liquid Propulsion*, 3-6 December 2002 – Liege, Belgium.
- [20] G.Z. Gershuni, D.V. Lyubimov, *Thermal Vibrational Convection*, John Wiley & Sons, New-York, 1998.
- [21] A. Jounet, Phys. Rev. E, 65, pp.37301–37304, 2002
- [22] S.V. Avdeev, A.I. Ivanov, A.V. Kalmykov, A.A. Gorbunov, S.A. Nikitin, V.I. Polezhaev, G.F. Putin, A.V. Zuzgin A.V., V.V. Sazonov, D. Beysens, Y. Garrabos, T. Fröhlich, B. Zappoli, *Experiments in the far and near critical fluid aboard the MIR station with the use of the 'Alice-1' instrument*, in Proceedings of the Joint Xth European and Vith Russian Symposium on Physical Science in Microgravity, St. Petersburg, Russia, 15-21 June 1997, Vol.1, pp.333–340, V.S. Avduyevsky and V.I. Polezhaev [Eds.], Institute for Problems in Mechanics, RAS, Moscow.
- [23] Y. Garrabos, D. Beysens, C. Chabot, R. Wunenburger, V. Polezhaev, V. Emelianov, A. Ivanov, A. Kalmykov, *Thermo-Convectional Phenomena Induced by Vibrations in Supercritical SF6 Under Low Gravity*, preprint, 2004.
- [24] S. Fauve, K. Kumar, C. Laroche, D. Beysens, Y. Garrabos, Phys. Rev. Lett. 68, pp.3160–3163, 1992.
- [25] R. Wunenburger, P. Evesque, C. Chabot, Y. Garrabos, S. Fauve, D. Beysens, Phys. Rev. E 59, pp.5440–5445, 1999.

- [26] D.V. Lyubimov, A. Cherepanov, *Izvestiya Akademii Nauk SSSR, Mekhanika Zhidkosti i Gaza* 6, 8-13, translated in *Fluid Dynamics* 86, pp.849–854, 1987.
- [27] D. Beysens, C. Chabot, Y. Garrabos, *Microgravity Sci. Technol.* 11, pp.113–118, 1998.
- [28] D. Beysens, D. Chatain, P. Evesque, Y. Garrabos, *Phase separation under vibrations in near-critical hydrogen free of gravity effects*, submitted, 2004.